Living fluids/Fluides vivants

Flow dynamics of red blood cells and their biomimetic counterparts

Dynamique sous écoulement des globules rouges et de leurs contreparties biomimétiques

Petia M. Vlahovska [a], Dominique Barthes-Biesel [b], Chaouqi Misbah [c,*]

[a] School of Engineering, Brown University, Providence, RI 02906, USA
[b] Biomécanique et bioingénierie, UMR CNRS 7338, Université de Technologie, CS60319, 60203 Compiègne, France
[c] Université Grenoble-1/CNRS, Laboratoire interdisciplinaire de physique/UMR 5588, 140, av. de la Physique, BP 87, 38402 Saint-Martin-d'Hères, France

A B S T R A C T

We review recent experimental, theoretical, and computational studies of red blood cells and their mimics, vesicles and capsules, in flow. We focus on the continuum approach in modeling cell deformability and blood rheology.

© 2013 Published by Elsevier Masson SAS on behalf of Académie des sciences.

R É S U M É

Nous passons en revue les progrès expérimentaux, théoriques et numériques réalisés dans l'étude de la dynamique des globules rouges et des systèmes biomimétiques, les vésicules et capsules sous écoulement. Nous mettons l'accent sur les approches continues de la modélisation de la déformabilité des cellules ainsi que sur la rhéologie du sang.

© 2013 Published by Elsevier Masson SAS on behalf of Académie des sciences.

1. Introduction

Red blood cells (RBCs) are micron-sized cells that are the main component of blood; they make up for about 45% of its volume. Blood circulates through the body via a network of vessels with diameter ranging from few microns in the microcirculation (e.g. capillaries), which is comparable to and even smaller than the RBC size, to few millimeters in the macrocirculation (e.g., aorta). Normal physiological function depends on the mechanical stability of the individual RBCs and, since blood is a dense suspension, on their collective dynamics under widely varying flow and geometry conditions. This is a vast area of active research, as evident from recent reviews [1–5]. Here we overview the work on this topic in recent years.

The healthy human RBC lacks nucleus and organelles; it is essentially a membrane encapsulating a hemoglobin solution. The membrane consists of a lipid bilayer supported by an attached spectrin polymer network (Fig. 1b). Features of the RBC mechanics arising from the properties of either the lipid bilayer or the spectrin network are studied on two model systems: vesicles (made of lipid bilayers) [6] and capsules (made of polymerized membranes) [7,8]. In this review we attempt to provide an overview of the understanding of the dynamics of real RBCs gained from these two model systems.

Since the composite bilayer-spectrin membrane is very thin ($\sim$10 nm [9]), on the length scale of the cell the membrane can be treated as a two-dimensional viscoelastic interface. Accordingly, continuum models based on elasticity theory and
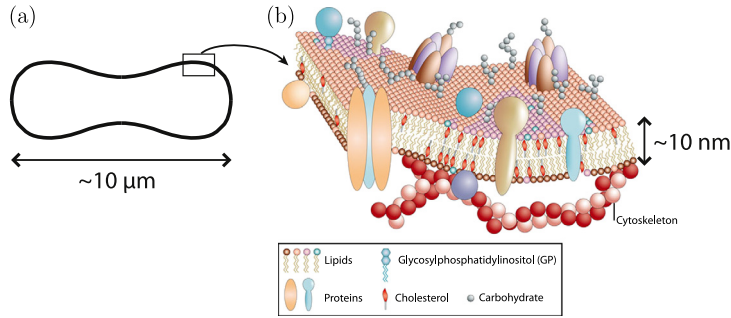
Fig. 1. Illustration of the continuum approach to modeling the human RBC membrane. (a) The equilibrium shape of a healthy human RBC is a biconcave disk approximately 8.0 μm in diameter and 2.0 μm in width. The (composite) cell membrane is approximated as a continuum viscoelastic interface. (b) The cell membrane structure comprises the lipid bilayer, the spectrin network and transmembrane proteins [12]. Color available in the online version of this article.

fluid dynamics provide a basis for studying RBC mechanics on mesoscopic to macroscopic length and time scales (Fig. 1). In this review we discuss only the continuum approaches. However, we should note that in recent years there is increasing interest in particle-based simulations. Such methods could potentially answer questions concerning the coupling of bio-chemistry and mechanics, which require resolution of subcellular structures and processes, for example shear-induced ATP release [5] and the mechanics of diseased RBCs [10]. We refer the interested reader to [11].

2. Membrane models

Under stress, energy is stored in the membrane through the elastic deformations (bending, shearing, and dilation/compression) or dissipated by viscous friction. The fluid lipid bilayer is responsible for the resistance to bending, stretching and viscous dissipation, while the spectrin scaffolding is responsible for the elastic behavior such as resistance to shearing (Fig. 1b).

The cost for bending is described by several models based on the Helfrich energy [13]. For a membrane patch with area A the bending energy E_b can be expressed as:

$$E_b = \frac{\kappa}{2} \oint_A (2H)^2 \, dA + \kappa_g \oint_A K_G \, dA \tag{1}$$

where κ and κ_g are the bending and the Gaussian elastic moduli, H and K_G are the mean and Gaussian curvatures. The contribution from the Gaussian curvature is a constant if the topology of the surface does not change.

A classic model for the elastic energy E_e associated with the stretch and shear of the spectrin polymer network is [14–16]:

$$E_e = \frac{K_A}{2} \oint \alpha^2 \, dA + \mu \oint \beta \, dA \tag{2}$$

where $\alpha = \lambda_1 \lambda_2 - 1$ and $\beta = (\lambda_1 - \lambda_2)^2 / 2\lambda_1\lambda_2$ are the local area and shear strain invariants and λ_1 and λ_2 are the local principal stretches. K_A and μ are the elastic moduli for stretch and shear, respectively. Higher-order nonlinear elastic terms can be included in the strain energy Eq. (2) to describe very deformed shapes such as echinocytes [17,18].

The mechanical properties of the RBC membrane have been measured by various techniques: micropipette aspiration [15], optical tweezers [19–23], electric field deformation [24,25] and thermal shape fluctuations (flickering) [26,27]. The surface shear elastic modulus μ is estimated to be a few μN/m, while the area expansion K_A (controlled by the lipid bilayer) is about 10^5 higher than that [4]; accordingly the membrane is virtually area-incompressible. The bending rigidity similar to that of lipid bilayers, in the order of a few $10 k_B T$ (here k_B is the Boltzmann constant and T is the absolute temperature).

Equilibrium RBC shapes minimize the sum of the bending and elastic energies (Eqs. (1) and (2)). However, the shapes under flow represent a non-equilibrium problem and energy minimization is not applicable; instead the cell shape and motion are determined by the balance of membrane and viscous flow stresses.

The membrane stresses per unit area of deformed membrane are obtained from the variation of bending and elastic energies. For example, Eq. (1) yields:

$$\boldsymbol{\tau}^\kappa = -\kappa \left(4H^3 - 4K_G H + 2\nabla_s^2 H\right) \mathbf{n} \tag{3}$$

The area-incompressibility constraint is treated by the use of a local Lagrange multiplier, which adds an additional term to the free energy of the membrane $\int \sigma \, dA$. The corresponding stress is:

$$\boldsymbol{\tau}^\sigma = \sigma H \mathbf{n} - \nabla_s \sigma \tag{4}$$

These forces can also be written as a surface divergence of a second-order stress tensor:

$$\boldsymbol{\Sigma} = -\kappa\left(-\frac{1}{2}H^2\mathbf{I}_s + H\nabla_s\mathbf{n} - \mathbf{n}\nabla_s H\right) + \sigma\mathbf{I}_s \tag{5}$$

The elastic behavior can be described by various constitutive laws [28,8], which for small membrane deformations reduce to a linear stress–strain relation (a two-dimensional equivalent of Hooke's law) [29,30]:

$$\boldsymbol{\tau}^\mu = 2(K_A - \mu)(\nabla_s \cdot \mathbf{d})H\mathbf{n} - (K_A - \mu)\nabla_s\nabla_s \cdot \mathbf{d} - \mu\nabla_s \cdot \left[\nabla_s\mathbf{d}\cdot\mathbf{I}_s + \mathbf{I}_s\cdot(\nabla_s\mathbf{d})^\dagger\right] \tag{6}$$

where $\mathbf{d}$ is the displacement of a material particle of the membrane from its unstressed position. The surface gradient operator is defined as $\nabla_s = \mathbf{I}_s \cdot \nabla$, where the matrix $\mathbf{I}_s = \mathbf{I} - \mathbf{nn}$ represents a surface projection. Like $\boldsymbol{\tau}^\kappa$, the elastic force can also be written as a surface divergence of a second-order stress tensor (see [30,7]). For an incompressible membrane $\nabla_s \cdot \mathbf{d} = 0$ and the elastic stresses depend only on the shear elastic resistance.

Membrane viscous stresses depend not on the strain but on the rate of strain; the analog of Eq. (6) for a Newtonian interface has the interface velocity $\mathbf{v}^m$ instead of $\mathbf{d}$, the surface shear viscosity η^{mm} in place of μ, and the surface dilational viscosity in place of K_A.

3. RBC dynamics: Experimental observations

3.1. Equilibrium fluctuations

Thermally induced membrane undulations are widely used to measure the mechanical properties (elastic moduli and viscosity) of artificial lipid bilayers [31,32]. The RBC membrane, however, shows some non-trivial features. Experiments find that the fluctuations are not isotropic on the RBC surface but enhanced at the outer convex region [33]. It appears that the RBC fluctuations are sensitive to ATP but this is an effect still under debate [34,27,33,23]. Another surprising result is that the RBC effective viscosity determined from fluctuation analysis is an order of magnitude higher than usually assumed [27], which is attributed to "unknown dissipative process".

3.2. Flow

In flows resembling the microcirculation, RBCs exhibit various behaviors. In steady shear flow, a RBC deforms into an ellipsoid that can tank-tread (the cell shape and orientation with respect to the flow direction remain steady, while the membrane rotates as a tank-tread), tumble (continuous flipping), or "swing" (tank-treading accompanied by oscillations in the inclination angle) [35]. Oscillatory shear may drive chaotic cell response, namely, irregular sequences of tumbling and tank-treading [36]. In capillary flows, an individual RBC can adopt either symmetric parachute or asymmetric slipper shape depending on confinement and flow rate [1,37]; multiple RBCs form clusters with limiting size, depending on the applied pressure drop (flow strength) [38].

Membrane-bound particles such as vesicles [2] and capsules [7,8] mimic some features of the RBCs behavior. For example, vesicles made of pure lipid bilayer can undergo tank-treading or tumbling in linear (shear) flows [39,40], and can adopt parachute- and slipper-shapes in quadratic (capillary) flows [41]. The swinging motion [42] and the parachute shape in pore flow [43,44] were also reported for capsules. Recent experiments showed that RBCs under shear flow can perform a rolling motion [45].

4. RBC dynamics: Modeling

The explanation of the experimentally observed behaviors of RBCs has been attempted with various theoretical approaches, including reduced analytical models and detailed numerical simulations.

4.1. Analytical models

Theoretical models for the dynamics of a deformable RBC simplify the cell shape and membrane rheology in order to derive an analytical solution. For example, shape fluctuations are studied on a planar interface because typically the undulation amplitude is much smaller than the curvature of the cell. The dynamics of the whole RBC in flow is studied by approximating its shape as an ellipsoid. The exact solutions provide physical insight and results that are useful to validate numerical simulations.

4.1.1. Fluctuations

Thermal fluctuations of a fluid membrane were considered in the classic studies by [46] in the case of a planar interface, and [47] – for a quasi-spherical vesicle. The curvature undulations of the membrane h_q with wave number q have time-averaged amplitude:

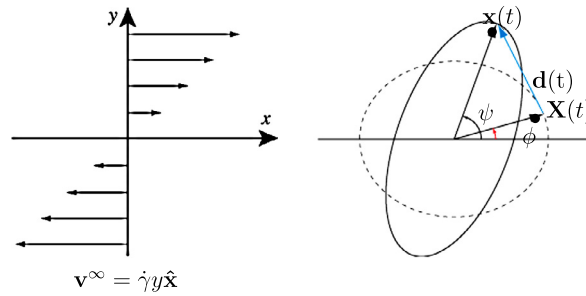$$\langle h_q^2\rangle \sim \frac{k_B T}{\kappa q^4 + \sigma q^2} \tag{7}$$

Fig. 2. Sketch of the flow and capsule configuration. ψ is the inclination angle of the capsule major axis, ϕ is the angle between the flow direction and the material particle in the reference configuration. The time rate of change of the phase angle $\psi - \phi$ is the tank-treading frequency of the membrane.

and evolve as $h_q \sim \exp(-st)$ with a relaxation rate $s = (\kappa q^3 + \sigma q)/4\eta$ reflecting the balance between energy storage in bending and energy dissipation by the viscosity of the surrounding fluid. The dynamics predicted by the classic theory, however, shows discrepancies with the experiments, e.g., higher bulk fluid viscosity is needed to fit the data [32]. Surface viscosity could potentially explain the experimental findings. A model for the dynamics of a planar membrane with surface viscosity has been recently accomplished [48,49] but not yet tested on vesicle fluctuation data. Actually, in planar geometry the out-of-plane (bending) and in-plane (shear) modes are decoupled, hence one needs to consider the dynamics of a quasi-spherical vesicle, i.e., generalize the Milner–Safran model [47] in order to see the effect of membrane viscosity.

The effect of the spectrin cytoskeleton can be included by treating the polymer network as a homogeneous viscoelastic shell coupled to the lipid bilayer [50,51]. However, the experimental observations discussed in Section 3.1 challenge the continuum view of the RBC membrane. The spectrin cytoskeleton is only sparsely connected to the lipid bilayer, and may be undergoing continuous remodeling (breaking and reforming of the network). Hence, nonthermal (ATP-driven) shape fluctuations may reflect topological defects induced in the cytoskeleton network by ATP [52].

4.1.2. Flow

The RBC dynamics under flow is studied using a "capsule" model: a nearly-spherical closed membrane. The capsule non-sphericity is characterized by the excess area Δ, which is the difference between the capsule area and the area of an equivalent volume sphere:

$$\Delta = \frac{A}{a^2} - 4\pi, \quad a = \left(\frac{3V}{4\pi}\right)^{1/3} \tag{8}$$

$\Delta = 0$ for a sphere, and $\Delta > 0$ otherwise. For red blood cells $\Delta \simeq 5$. Dimensional analysis of the governing equations shows that RBC dynamics are controlled by several dimensionless parameters. One subset depends solely on cell geometry and fluid properties: excess area Δ and viscosity ratio between the encapsulated and suspending fluids $\lambda = \eta_{in}/\eta_{ex}$. The rest are flow-dependent: capillary number based on the bending rigidity $Ca_\kappa = \eta_{ex} a^3 \dot{\gamma}/\kappa$, and capillary number based on the shear elasticity $Ca_\mu = \eta_{ex} a \dot{\gamma}/\mu$, where $\dot{\gamma}$ is the shear rate. In the case of Poiseuille flow, the curvature of the flow is another relevant parameter.

In the case of pure lipid bilayer (shear-free interface), the theoretical phase diagram of vesicle behaviors (tank-treading, tumbling, breathing) depends on 3 control parameters, Δ, λ, and Ca_κ [53–56]. The phase diagram is supported by numerical simulations [57,58], but questioned by experiments [40]. The discrepancies in the latter case appear to be due to membrane thermal undulations, which are not included in the model. Note also that addition of fluorophores in high-enough concentrations (as in the aforementioned experiments [40]) in membranes are known to significantly alter membrane properties, in that pore formation can take place [59] leading to permanent flow between inside and outside the vesicle. Further studies are needed in order to see whether thermal fluctuations or pore formation are the determinant factor. Further analysis of vesicle dynamics highlighted that tumbling can be suppressed by slippage between the two monolayers [60], application of a uniform electric field in the velocity gradient direction [61] or even small amounts of inertia [62]. Recently, the original model of vesicles under shear flow [53,54] has been solved exactly [63].

The small-deformation asymptotic theory has been applied to study vesicles in Poiseuille flow [64] or sedimentation [65]. Intriguingly, despite the axial symmetry of the ambient flow, non-axisymmetric solutions for the vesicle shapes are possible. For example, in Poiseuille flow, in addition to centered symmetric (parachute or bullet) shapes, off-centered asymmetric (slipper) shapes exist at low flow strengths. These findings are in agreement with numerical simulations [66]. However, the asymmetric slippers are elusive in experiments [41]. As discussed in [67] the experimentally explored parameter range is beyond the regime of existence of the slipper shape. Highly deflated vesicles (as is the case with RBCs) should favor the emergence of slipper shape. While the problem for cell shapes and dynamics in capillary flows is far from being fully solved, the analytical results suggest that neither the cytoskeleton nor the confinement due to channel walls is essential for the appearance of the slipper.

As an example of the successful application of the analytical approach to gain physical insight, here we summarize the analysis of the swinging motion of a RBC in shear flow, which has generated some controversy. Phenomenological models [35,68–70], which approximates the RBC with an ellipsoid of *fixed* shape, predicted intermittent behavior (swinging periodically interrupted by a tumble), for which no evidence was found in the numerical simulations [71–73]. A *deformable* cell was considered in the treatment by [74–76]. Vlahovska et al. [74] described the capsule dynamics in terms of the orientation angle between its major axis and the flow direction, ψ, and a parameter R, which measures the ellipticity of the cell contour in the x–y plane, see Fig. 2. The non-sphericity of the rest shape is measured by $\epsilon_0 = R$ $(t = 0)$:

$$\frac{\partial \psi}{\partial t} = -\frac{1}{2} + \frac{\Lambda^{-1}}{2R} \cos(2\psi) + \epsilon_0 \frac{(S\Lambda)^{-1}}{2R} \sin(2\phi - 2\psi) \tag{9}$$

$$\frac{\partial R}{\partial t} = \Lambda^{-1}(1 - R^2)\sin(2\psi) + (S\Lambda)^{-1}\left\{\epsilon_0(1 - R^2)\cos(2\phi - 2\psi) - R\sqrt{(1 - R^2)(1 - \epsilon_0^2)}\right\} \tag{10}$$

where

$$S^{-1} = \sqrt{\frac{2\Delta}{15\pi}} Ca_\mu^{-1}, \qquad \Lambda = \frac{\sqrt{\Delta}(23\lambda + 32)}{8\sqrt{30\pi}} \tag{11}$$

The tank-treading frequency is $\partial_t \phi = -1/2$, where ϕ is the angle between the position vector of a material particle and the flow direction. Eqs. (9) and (10) reduce to the vesicle model if the shear elasticity is zero, i.e., $S^{-1} = 0$. The capsule model predicts the observed transition from tumbling to swinging as the shear rate increases. Near the transition, intermittent behavior (swinging periodically interrupted by a tumble) is found only if the capsule deforms in the shear plane and does not undergo stretching or compression along the vorticity direction; the intermittency disappears if deformation along the vorticity direction occurs, i.e., if the capsule "breathes".

4.2. Computational models

In the case of large deformations, it is necessary to resort to numerical models. The usual technique of resolution consists in injecting the undeformed particle in the flow field and in following numerically the time evolution of the particle motion and deformation until a steady state is reached, if any. At a given time, the position of the membrane material points is thus known. By comparison with the initial reference state, the deformation, curvature and stress in the membrane $\boldsymbol{\tau}^m = \boldsymbol{\tau}^\kappa + \boldsymbol{\tau}^\mu + \boldsymbol{\tau}^\sigma$ are easily computed. Then, the solution of the flow equations gives the velocity $\mathbf{v}^m$ of the membrane points, which can be integrated to give the new position of the membrane material points, and the process is repeated. Different numerical techniques have been used, but the general principle is the same.

One technique is based on the boundary integral method which applies to low Reynolds number flows (Stokes flows) and which consists in recasting the flow equations of motion in integral form. For the particular case where the viscosity of the two liquids are equal, $\lambda = 1$, the membrane velocity is given by [77]:

$$\mathbf{v}^m = \mathbf{v}^\infty - \frac{1}{8\pi \eta^{\mathrm{ex}}} \oint_A (\mathbf{G} \cdot \boldsymbol{\tau}^m) \, dA \tag{12}$$

where $\mathbf{G}$ is the Green's function for the Stokes equations, and $\mathbf{v}^\infty$ is the applied flow (the formulation for different viscosity fluids is a bit more cumbersome). The integration is performed on the particle deformed surface A at time t. Within the framework of this integral representation, the fluid and solid equations of motion can then be solved on the same grid, thus reducing the geometric dimension of the problem by one. This technique has been used extensively over the years [78–82] and has been shown to be very precise. It is however, restricted to Stokes flows and thus excludes inertial or non-Newtonian effects. In the case of capsules it has allowed to compute the flow of initially ellipsoidal capsules and show how the tumbling and swinging regimes depended on the capsule initial aspect ratio, membrane law and flow strength [83]. It is also possible to use this technique to compute the flow of an initially spherical capsule in a small pore with a square or circular cross section [84].In this case a parachute or slug profile is found depending on flow strength and confinement ratio.

In the case of RBC, a major challenge is to enforce the local inextensibility of the membrane; it results in a very stiff problem with high computational cost. Recently efficient schemes for the BIM have been developed to study pure lipid vesicles (shear-free interface $\mu = 0$) [58,85–89], multicomponent membrane vesicles [90], and RBCs [91,92]. These computations have allowed to explore the behavior of an isolated vesicle in wall-bounded shear flows [85], unbounded quadratic flows [66,67], and capillary flows [93]. Collective dynamics of many vesicles has also been considered [94,95], but only to a limited extent, and a systematic numerical study of suspension rheology is still lacking despite recent progress in this direction with capsules [96]. Such simulations are needed to interpret the experiments on hydrodynamic interactions between vesicles [97] and the effective viscosity of suspensions of RBCs and vesicles [98], which was found to depend non-monotonically on λ.

A great advantage of the BIM is the accurate computation of the interface evolution. However, the method cannot handle topological changes such as budding, and it is restricted to zero-Reynolds number (no inertia). To treat these effects, other computational approaches are being developed, e.g., level-set [99,100], phase-field [101], and front-tracking [102,103].

A simulation using the level-set method recently showed that inertia suppresses vesicle tumbling in simple shear flow [62]. Another computational challenge is to include the membrane thermal undulations; progress in this direction has been made only for planar membranes [104–106].

5. Conclusions

Despite decades of intense research, the dynamic behavior of RBCs remains an active research area full of open problems such as shape fluctuations with account for ATP effects or membrane viscosity, hydrodynamic interactions and clustering of RBCs and the rheology of dense suspensions. Finally, the mechanics of diseased RBCs, e.g., in sickle cell anemia or malaria, is another virtually unexplored problem. This review provides the continuum perspective in analyzing RBC dynamics, however particle-based methods are becoming increasingly popular [11]. The two approaches complement each other and their potential fusion could lead to multi-scale models that more closely represent the real RBC and microcirculatory flows.

Acknowledgements

References

[1] M. Abkarian, M. Faivre, R. Horton, K. Smistrup, C.A. Best-Popescu, H.A. Stone, Cellular-scale hydrodynamics, Biomed. Mater. 3 (2008) 034011.
[2] M. Abkarian, A. Viallat, Vesicles and red blood cells in shear flow, Soft Matter 4 (2008) 653–657.
[3] P.M. Vlahovska, T. Podgorski, C. Misbah, Vesicles and red blood cells: From individual dynamics to rheology, C. R. Physique 10 (2009) 775–789.
[4] S. Guido, G. Tomaiuolo, Microconfined flow behavior of red blood cells in vitro, C. R. Physique 10 (2009) 751–763.
[5] J. Wan, A.M. Forsyth, H.A. Stone, Red blood cell dynamics: From cell deformation to atp release, Integr. Biol. 3 (2011) 972–981.
[6] U. Seifert, Configurations of fluid membranes and vesicles, Adv. Phys. 46 (1997) 13–137.
[7] D. Barthes-Biesel, Capsule motion is flow: Deformation and membrane buckling, C. R. Physique 10 (2010) 764–774.
[8] D. Barthes-Biesel, Modeling the motion of capsules in flow, Curr. Opin. Colloid Interface Sci. 16 (2011) 3–12.
[9] N. Mohandas, E. Evans, Mechanical properties of the red cell membrane in relation to molecular structure and genetic defects, Annu. Rev. Biophys. Biomol. Struct. 23 (1994) 787–818.
[10] S. Suresh, Mechanical response of human red blood cells in health and disease: Some structure-property-function relationships, J. Mater. Res. 21 (2006) 1871–1877.
[11] X. Li, P.M. Vlahovska, G.E. Karniadakis, Continuum- and particle-based modeling of shapes and dynamics of red blood cells in health and disease, Soft Matter 9 (2013) 28–37, http://dx.doi.org/10.1039/c2sm26891d.
[12] http://www.nature.com/horizon/livingfrontier/background/figs/membrane_f2.html.
[13] W. Helfrich, Elastic properties of lipid bilayers – theory and possible experiments, Z. Naturforsch. 28c (1973) 693–703.
[14] E.A. Evans, R. Skalak, Mechanics and Thermodynamics of Biomembranes, CRC Press, Boca Raton, Florida, 1980.
[15] E.A. Evans, Structure and deformation properties of red blood cells: Concepts and quantitative methods, in: S. Fleischer, B. Fleischer (Eds.), Methods in Enzymology, vol. 173, Academic Press, 1989, pp. 3–35.
[16] R. Mukhopadhyay, H.W.G. Lim, M. Wortis, Echinocyte shapes: Bending, stretching, and shear determine bump shape and spacing, Biophys. J. 82 (2002) 1756–1772.
[17] H.W.G. Lim, M. Wortis, R. Mukhopadhyay, Stomatocyte–discocyte–echinocyte sequence of the human red blood cell: Evidence for the bilayer-couple hypothesis from membrane mechanics, Proc. Natl. Acad. Sci. USA 99 (2002) 16766–16769.
[18] K. Khairy, J. Howard, Minimum-energy vesicle and cell shapes calculated using spherical harmonics parameterization, Soft Matter 7 (2011) 2138–2143.
[19] G. Lenormand, S. Henon, A. Richert, J. Simeon, F. Gallet, Irect measurement of the area expansion and shear moduli of the human red blood cell membrane skeleton, Biophys. J. 81 (2001) 43–56.
[20] S. Henon, G. Lenormand, A. Richert, J. Simeon, F. Gallet, A new determination of the shear modulus of the human erythrocyte membrane using optical tweezers, Biophys. J. 76 (1999) 1145–1151.
[21] M. Dao, C. Lim, S. Suresh, Mechanics of the human red blood cell deformed by optical tweezers, J. Mech. Phys. Solids 51 (2003) 2259–2280.
[22] A.T. Brown, J. Kotar, P. Cicuta, Active rheology of phospholipid vesicles, Phys. Rev. E 84 (2011) 021930.
[23] Y. Yoon, J. Kotar, A.T. Brown, P. Cicuta, Red blood cell dynamics: From spontaneous fluctuations to non-linear response, Soft Matter 7 (2011) 2042–2051.
[24] H. Engelhardt, E. Sackmann, On the measurement of shear elastic moduli and viscosities of erythrocyte plasma membranes by transient deformation in high frequency electric fields, Biophys. J. 54 (1988) 495–508.
[25] R.S. Gracia, N. Bezlyepkina, R.L. Knorr, R.L. Lipowsky, R. Dimova, Effect of cholesterol on the rigidity of saturated and unsaturated membranes: Fluctuation and electrodeformation analysis of giant vesicles, Soft Matter 6 (2010) 1472–1482.
[26] Y. Park, C.A. Best, K. Badizadegan, R. Dasari, M.S. Feld, T. Kuriabova, M.L. Henle, A.J. Levine, G. Popescu, Measurement of red blood cell mechanics during morphological changes, Proc. Natl. Acad. Sci. USA 107 (2010) 6731–6736.
[27] T. Betz, M. Lenz, J.-F. Joanny, C. Sykes, Atp-dependent mechanics of red blood cells, Proc. Natl. Acad. Sci. USA 106 (2009) 15320–15325.
[28] C. Pozrikidis, Modeling and Simulation of Capsules and Biological Cells, CRC Press, 2003.
[29] D. Barthes-Biesel, J.M. Rallison, The time-dependent deformation of a capsule freely suspended in a linear shear flow, J. Fluid Mech. 113 (1981) 251–267.
[30] D.A. Edwards, H. Brenner, D.T. Wasan, Interfacial Transport Processes and Rheology, Butterworth-Heinemann, 1991.
[31] V. Vitkova, C. Misbah, Dynamics of lipid vesicles – from thermal fluctuations to rheology, in: A. Iglic (Ed.), Advances in Planar Lipid Bilayers and Liposomes, vol. 14, Elsevier, 2011, pp. 257–292.
[32] T. Betz, C. Sykes, Time resolved membrane fluctuation spectroscopy, Soft Matter 8 (2012) 5317–5326.
[33] Y.-K. Park, C.A. Best, T. Auth, N.S. Gov, S.A. Safran, G. Popescu, S. Suresh, M.S. Feld, Metabolic remodeling of the human red blood cell membrane, Proc. Natl. Acad. Sci. USA 107 (2010) 1289–1294.

[34] J. Evans, W. Gratzer, N. Mohandas, K. Parker, J. Sleep, Fluctuations of the red blood cell membrane: Relation to mechanical properties and lack of atp dependence, Biophys. J. 94 (2008) 4134–4144.
[35] M. Abkarian, M. Faivre, A. Viallat, Swinging of red blood cells under shear flow, Phys. Rev. Lett. 98 (2007) 188302.
[36] J. Dupire, M. Abkarian, A. Viallat, Chaotic dynamics of red blood cells in a sinusoidal flow, Phys. Rev. Lett. 104 (2010) 168101.
[37] G. Tomaiuolo, M. Simeone, V. Martinelli, B. Rotoli, S. Guido, Red blood cell deformation in microconfined flow, Soft Matter 5 (2009) 3736–3740.
[38] G. Tomaiuolo, L. Lanotte, G. Ghigliotti, C. Misbah, S. Guido, Red blood cell clustering in Poiseuille microcapillary flow, Phys. Fluids 24 (2012) 051903.
[39] J. Deschamps, V. Kantsler, V. Steinberg, Phase diagram of single vesicle dynamical states in shear flow, Phys. Rev. Lett. 102 (2009) 118105.
[40] N.J. Zabusky, E. Segre, J. Deschamps, V. Kantsler, V. Steinberg, Dynamics of vesicles in shear and rotational flows: Modal dynamics and phase diagram, Phys. Fluids 23 (2011) 041905.
[41] G. Coupier, A. Farutin, C. Minetti, C. Misbah, Shape diagram of vesicles in Poiseuille flow, Phys. Rev. Lett. 108 (2012) 178106.
[42] A. Walter, H. Rehage, H. Leonhard, Shear induced deformation of microcapsules: Shape oscillations and membrane folding, Colloids Surf. A 183–185 (2001) 123–132.
[43] Y. Lefebvre, E. Leclerc, D. Barthès-Biesel, J. Walter, F. Edwards-Lévy, Flow of artificial microcapsules in microfluidic channels: A method for determining the elastic properties of the membrane, Phys. Fluids 20 (12) (2008) 123102, http://dx.doi.org/10.1063/1.3054128, http://link.aip.org/link/PHFLE6/v20/i12/p123102/s1&Agg=doi.
[44] T.X. Chu, a V. Salsac, E. Leclerc, D. Barthès-Biesel, H. Wurtz, F. Edwards-Lévy, Comparison between measurements of elasticity and free amino group content of ovalbumin microcapsule membranes: Discrimination of the cross-linking degree, J. Colloid Interface Sci. 355 (1) (2011) 81–88, http://dx.doi.org/10.1016/j.jcis.2010.11.038, http://www.ncbi.nlm.nih.gov/pubmed/21194705.
[45] J. Dupire, M. Socol, A. Viallat, Full dynamics of a red blood cell in shear flow, PNAS 109 (2012) 20808.
[46] F. Brochard, J.F. Lennon, Frequency spectrum of the flicker phenomenon in erythrocytes, J. Phys. (France) 36 (1975) 1035–1047.
[47] S.T. Milner, S.A. Safran, Dynamical fluctuations of droplet microemulsions and vesicles, Phys. Rev. A 36 (1987) 4371–4379.
[48] M.C. Watson, F.L.H. Brown, Interpreting membrane scattering experiments at the mesoscale: The contribution of dissipation within the bilayer, J. Chem. Phys. 98 (2010) L9–L11.
[49] M.C. Watson, Y. Peng, Y. Zheng, F.L.H. Brown, The intermediate scattering function for lipid bilayer membranes: From nanometers to microns, J. Chem. Phys. 135 (2011) 194701.
[50] A. Levine, F. MacKintosh, Dynamics of viscoelastic membranes, Phys. Rev. E 66 (2002) 061606.
[51] S.B. Rochal, V.L. Lorman, G. Mennessier, Viscoelastic dynamics of spherical composite vesicles, Phys. Rev. E 71 (2005) 021905.
[52] S.A. Safran, N. Gov, A. Nicolas, U.S. Schwarz, T. Tlusty, Physics of cell elasticity, shape and adhesion, Physica A 352 (2005) 171–201.
[53] C. Misbah, Vacillating breathing and tumbling of vesicles under shear flow, Phys. Rev. Lett. 96 (2006) 028104.
[54] P.M. Vlahovska, R. Gracia, Dynamics of a viscous vesicle in linear flows, Phys. Rev. E 75 (2007) 016313.
[55] V.V. Lebedev, K.S. Turitsyn, S.S. Vergeles, Nearly spherical vesicles in an external flow, New J. Phys. 10 (2008) 043044.
[56] B. Kaoui, A. Farutin, C. Misbah, Vesicles under simple shear flow: Elucidating the role of relevant control parameters, Phys. Rev. E 80 (2009) 061905.
[57] A. Farutin, T. Biben, C. Misbah, Analytical progress in the theory of vesicles under linear flow, Phys. Rev. E 81 (2010) 061904.
[58] T. Biben, A. Farutin, C. Misbah, Three-dimensional vesicles under shear flow: Numerical study of dynamics and phase diagram, Phys. Rev. E 83 (2011) 031921.
[59] O. Sandre, L. Moreaux, F. Brochard-Wyart, Dynamics of ransient pores in stretched vesicles, Proc. Natl. Acad. Sci. 96 (1999) 10591–10596.
[60] J. Schwalbe, P.M. Vlahovska, M. Miksis, Monolayer slip effects on the dynamics of a lipid bilayer vesicle in a viscous flow, J. Fluid Mech. 647 (2010) 403–419.
[61] J. Schwalbe, P.M. Vlahovska, M. Miksis, Vesicle electrohydrodynamics, Phys. Rev. E 83 (2011) 046309.
[62] A. Laadhari, P. Saramito, C. Misbah, Vesicle tumbling inhibited by inertia, Phys. Fluids 24 (2012) 031901.
[63] M. Guedda, M. Abaidi, M. Benlahsen, C. Misbah, Dynamic modes of quasispherical vesicles: Exact analytical solutions, Phys. Rev. E 86 (2012) 051915.
[64] A. Farutin, C. Misbah, Symmetry breaking of vesicle shapes in Poiseuille flow, Phys. Rev. E 84 (2011) 011902.
[65] G. Boedec, M. Jaeger, M. Leonetti, Settling of a vesicle in the limit of quasispherical shapes, J. Fluid Mech. 690 (2012) 227–261.
[66] B. Kaoui, C. Misbah, Why do red blood cells have asymmetric shapes even in a symmetric flow? Phys. Rev. Lett. 103 (2009) 188101.
[67] B. Kaoui, N. Tahiri, T. Biben, C. Misbah, Complexity of vesicle microcirculation, Phys. Rev. E 84 (2011) 041906.
[68] J.M. Skotheim, T.W. Secomb, Red blood cells and other nonspherical capsules in shear flow: Oscillatory dynamics and the tank-treading-to-tumbling transition, Phys. Rev. Lett. 98 (2007) 078301.
[69] S. Kessler, R. Finken, U. Seifert, Elastic capsules in shear flow: Analytical solutions for constant and time-dependent shear rates, Eur. Phys. J. E 29 (2009) 399–413.
[70] H. Noguchi, Swinging and synchronized rotations of red blood cells in simple shear flow, Phys. Rev. E 80 (2009) 021902.
[71] S. Kessler, R. Finken, U. Seifert, Swinging and tumbling of elastic capsules in shear flow, J. Fluid Mech. 605 (2008) 207–226.
[72] Y. Sui, Y.T. Chew, P. Roy, Y.P. Cheng, H.T. Low, Dynamic motion of red blood cells in simple shear flow, Phys. Fluids 20 (2008) 112106.
[73] P. Bagchi, R.M. Kalluri, Dynamics of nonspherical capsules in shear flow, Phys. Rev. E 80 (2009) 016307.
[74] P.M. Vlahovska, Y.-N. Young, G. Danker, C. Misbah, Dynamics of a non-spherical microcapsule with incompressible interface in shear flow, J. Fluid Mech. 678 (2011) 221–247.
[75] S.S. Vergeles, P.E. Vorobev, Motion of near-spherical micro-capsule in planar external flow, JETP Lett. 94 (2011) 513–518.
[76] R. Finken, S. Kessler, U. Seifert, Micro-capsules in shear flow, J. Phys. Condens. Matter 23 (2011) 184113.
[77] C. Pozrikidis, Boundary Integral and Singularity Methods for Linearized Viscous Flow, Cambridge University Press, 1992.
[78] S. Ramanujan, C. Pozrikidis, Deformation of liquid capsules enclosed by elastic membranes in simple shear flow: Large deformations and the effect of capsule viscosity, J. Fluid Mech. 361 (1998) 117–143.
[79] A. Diaz, N.A. Pelekasis, D. Barthès-Biesel, Transient response of a capsule subjected to varying flow conditions: Effect of internal fluid viscosity and membrane elasticity, Phys. Fluids 12 (2000) 948–957.
[80] E. Lac, D. Barthès-Biesel, N.A. Pelekasis, J. Tsamopoulos, Spherical capsules in three-dimensional unbounded Stokes flow: Effect of the membrane constitutive law and onset of buckling, J. Fluid Mech. 516 (2004) 303–334.
[81] W.R. Dodson III, P. Dimitrakopoulos, Spindles, cusps, and bifurcation for capsules in Stokes flow, Phys. Rev. Lett. 101 (20) (2008) 208102, http://dx.doi.org/10.1103/PhysRevLett.101.208102.
[82] J. Walter, A.-V. Salsac, D. Barthes-Biesel, P. Le Tallec, Coupling of finite element and boundary integral methods for a capsule in a Stokes flow, Int. J. Numer. Methods Eng. 83 (2010) 829–850.
[83] J. Walter, A.-V. Salsac, D. Barthès-Biesel, Ellipsoidal capsules in simple shear flow: prolate versus oblate initial shapes, J. Fluid Mech. 676 (2011) 318–347.
[84] X. Hu, A.-V. Salsac, D. Barthès-Biesel, Flow of a spherical capsule in a pore with circular or square cross-section, J. Fluid Mech. 705 (2012) 176–194.
[85] H. Zhao, A.P. Spann, E.S.G. Shaqfeh, The dynamics of a vesicle in a wall-bound shear flow, Phys. Fluids 23 (2011) 121901.
[86] G. Boedec, M. Leonetti, M. Jaeger, 3d vesicle dynamics simulations with a linearly triangulated surface, J. Comput. Phys. 230 (2011) 1020–1034.
[87] S.K. Veerapaneni, A. Rahimian, G. Biros, D. Zorin, A fast algorithm for simulating vesicle flows in three dimensions, J. Comput. Phys. 230 (2011) 5610–5634.

[88] S. Veerapaneni, D. Gueyffier, G. Biros, D. Zorin, A numerical method for simulating the dynamics of 3d axisymmetric vesicles suspended in viscous flows, J. Comput. Phys. 228 (2009) 7233–7249.

[89] A. Rahimian, S.K. Veerapaneni, G. Biros, Dynamic simulation of locally inextensible vesicles suspended in an arbitrary two-dimensional domain, a boundary integral method, J. Comput. Phys. 229 (2010) 6466–6484.

[90] J. Sohn, Y. Tseng, S. Li, A. Voigt, J. Lowengrub, Dynamics of multicomponent vesicles in a viscous fluid, J. Comput. Phys. 229 (2010) 119–144.

[91] H. Zhao, A. Isfahani, L. Olson, J. Freund, A spectral boundary integral method for flowing blood cells, J. Comput. Phys. 229 (2010) 3726–3744.

[92] W.R. Dodson, P. Dimitrakopoulos, Tank-treading of erythrocytes in strong shear flows via a nonstiff cytoskeleton-based continuum computational modeling, Biophys. J. 99 (2010) 2906–2916.

[93] B. Kaoui, J. Harting, C. Misbah, Two-dimensional vesicle dynamics under shear flow: Effect of confinement, Phys. Rev. E 83 (2011) 066319.

[94] G. Ghigliotti, A. Rahimian, G. Biros, C. Misbah, Vesicle migration and spatial organization driven by flow line curvature, Phys. Rev. Lett. 106 (2011) 028101.

[95] H. Zhao, E.S.G. Shaqfeh, V. Narsimhan, Shear-induced particle migration and margination in a cellular suspension, Phys. Fluids 24 (2012) 011902.

[96] J.R. Clausen, D.A. Reasor, C.K. Aidun, The rheology and microstructure of concentrated non-colloidal suspensions of deformable capsules, J. Fluid Mech. 685 (2011) 202–234.

[97] M. Levant, J.A.E. Deschamps, Characteristic spatial scale of vesicle pair interactions in a plane linear flow, Phys. Rev. E 85 (2012) 056306.

[98] V. Vitkova, M. Mader, B. Polack, C. Misbah, T. Podgorski, Micro–macro link in rheology of erythrocyte and vesicle suspensions, Biophys. J. 95 (6) (2008) L33–L35.

[99] D. Salac, M. Miksis, A level set projection model of lipid vesicles in general flows, J. Comput. Phys. 230 (2011) 8192–8215.

[100] E. Maitre, C. Misbah, P. Peyla, A. Raoult, Comparison between advected-field and level-set methods in the study of vesicle dynamics, Physica D 241 (2012) 1146–1157.

[101] Q. Du, C. Liu, X. Wang, Simulating the deformation of vesicle membranes under elastic bending energy in three dimensions, J. Comput. Phys. 212 (2006) 757–777.

[102] A.Z.K. Yazdani, P. Bagchi, Phase diagram and breathing dynamics of a single red blood cell and a biconcave capsule in dilute shear flow, Phys. Rev. E 84 (2011) 026314.

[103] A.Z.K. Yazdani, R.M. Kalluri, P. Bagchi, Tank-treading and tumbling frequencies of capsules and red blood cells, Phys. Rev. E 83 (2011) 046305.

[104] P. Atzberger, P. Kramer, C. Peskin, A stochastic immersed boundary method for fluid-structure dynamics at microscopic length scales, J. Comput. Phys. 224 (2007) 1255–1292.

[105] P.J. Atzberger, Stochastic Eulerian Lagrangian methods for fluid-structure interactions with thermal fluctuations, J. Comput. Phys. 230 (2011) 2821–2837.

[106] F.L.H. Brown, Continuum simulations of biomembrane dynamics and the importance of hydrodynamic effects, Q. Rev. Biophys. 44 (2011) 391–432.